Supporting Information

Argaw *et al.* 10.1073/pnas.0808698106

SI Materials and Methods

Antibodies. CLN-3 (rabbit), CLN-5 (mouse, rabbit), CLN-12, OCLN, JAM-1, CASK, cingulin, ZO-1 (all rabbit), and GFAP (rat), were from Invitrogen. OCLN (goat) and VEGF-A (rabbit) were from Santa Cruz Biotechnology. CLN-12 (rabbit) and albumin (sheep) were from Abcam. Fibrinogen (rabbit) and Factor VIII-related antigen (mouse), were from Dako Cytomation.

Nucleofection. pDCLN5 or pSOCLN (1 μg) or empty vector controls were nucleofected into BMVEC cultures or control cell lines, using the Amaxa nucleofector program T05 (Amaxa).

Real-Time PCR. RNA was harvested using an Absolutely-RNA RT-PCR Miniprep Kit (Stratagene), cDNA was generated, and real-time PCR performed and validated as described (1). Primer sequences are available upon request.

Western Blotting. SDS/PAGE and Western blotting were performed as reported (1). For densitometry, nonsaturated developed films were scanned using a Canon LiDE scanner (Canon USA) and mean pixel density of each band measured using ImageJ 1.30 software (National Institutes of Health). Measurements were standardized to actin loading control, and fold change vs. control was calculated.

ELISA. Sandwich ELISA for VEGF-A was carried out using a commercial assay (R&D Systems).

CNS Microinjection. Mice (C57BL/6, 12 wk, at least 3 per condition per timepoint) were anesthetized and placed into a stereotactic frame (David Kopf Instruments). Mouse $VEGF_{165}$ (60 ng, in 3μL of PBS/BSA vehicle) or vehicle control was slowly microinjected into the cerebral cortex at $y = 1$ mm caudal to Bregma, $x = 2$ mm, $z = 1.5$ mm, as described (1). All studies were approved by the appropriate Institutional Review Board..

Experimental Autoimmune Encephalomyelitis. EAE was induced in C57BL/6 mice (8 wk, at least 5 per group per experiment) using immunization with $MOG_{35–55}$ peptide (Invitrogen), as reported (2). The day after the last injection of MOG was considered day 1. Clinical signs were scored as follows (2): 0, no symptoms; 1, floppy tail; 2, hind limb weakness/paraparesis; 3, hind limb paralysis/paraplegia; 4, forelimb and hind limb paralysis; 5, death. All studies were approved by the appropriate Institutional Review Board.

Immunocytochemistry. Cultures were fixed and stained as published (1) unless noted. For claudins, cells were fixed in 95% ethanol at 4 °C for 30 min, then 1:1 methanol/acetone for 1 min at room temperature. Primary antibodies were used at 1:100 except CLN-5 (1:50). Cultures were examined using an LSM 510 META confocal on an Axiovert 200 microscope (Carl Zeiss). Z-series stacks were collected using 0.5 μm on the z-axis.

Morphometric Analysis. Morphometric analyses were performed using ImageJ 1.30 software. Pixels positive for CLN-5, OCLN, fibrinogen, and albumin immunoreactivity were counted in projections of Z series stacks with the same number of images, from 5 separate animals with EAE, and 5 age- and sex-matched normal controls, at least 5 random 20× fields in 5 sections per animal from lumbar spinal cord by a blinded observer. EAE samples were from animals with paraparesis/paraplegia, 15–18 d postinduction.

1. Argaw T, *et al.* (2006) Interleukin-1β induces blood–brain barrier permeability via reactivation of the hypoxia-angiogenesis program. *J Immunol* 177:5574–5584.

2. Chen L, Brosnan CF (2006) Exacerbation of experimental autoimmune encephalomyelitis in P2X7R−/− mice: Evidence for loss of apoptotic activity in lymphocytes. *J Immunol* 176:3115–3126.

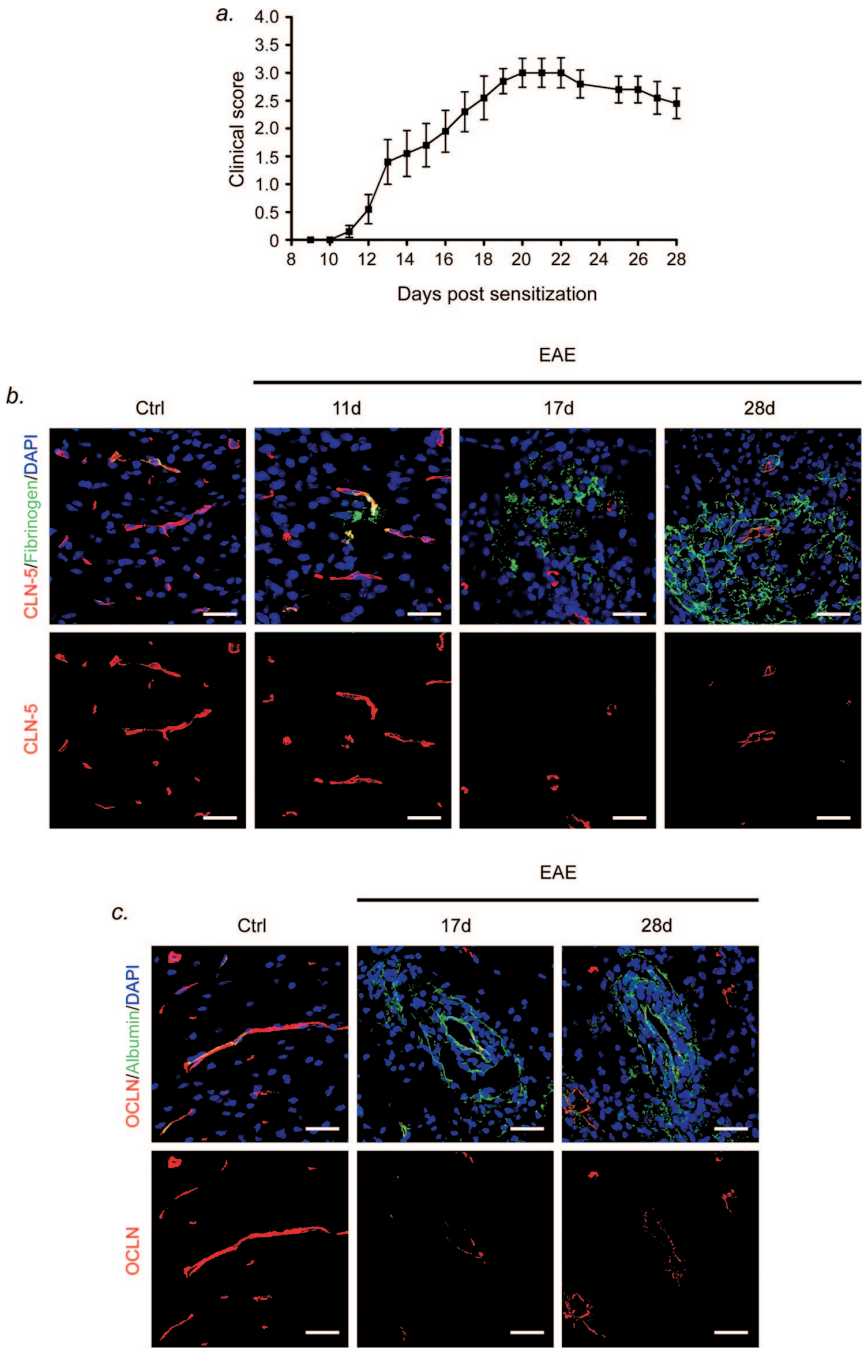

Fig. S1. Persistent BBB breakdown and disruption of CLN-5 and OCLN in EAE. (*A*) Clinical course of EAE induced in C57BL/6 mice (8 weeks) using $MOG_{35–55}$. Symptoms characterized by an ascending flaccid paralysis [Chen L, Brosnan CF (2006) Exacerbation of experimental autoimmune encephalomyelitis in P2X7R-/- mice: evidence for loss of apoptotic activity in lymphocytes. *J Immunol* 176:3115–3126.] (scored as described in *Materials and Methods*) are apparent from 10–12 d after induction and persist through 28–30 d. Results shown are from a single experiment in which EAE was induced in 5 age- and sex-matched animals, and are representative of 3 independent experiments. (*B* and *C*) Confocal Z-series projections of ventrolateral lumbar spinal cord from mice killed at clinical onset of EAE (10–12 d), and during the acute clinical phase (15–18 d) and more chronic clinical plateau (28–30 d). Sections were immunostained for CLN-5 plus fibrinogen (*B*) or OCLN plus albumin (*C*). BBB breakdown was mild at onset of clinical signs (*B*) and more widespread at 15–18 d, and persisted at 28–30 d (*B* and *C*). Importantly, BBB disruption at 28–30 d was accompanied by a persistent reduction in CLN-5 and OCLN (*B* and *C*, *Right*). The red channel (CLN-5 or OCLN) is presented below each image for clarity in *B* and *C*. Results shown are representative of findings from 3 independent experiments, 5 animals per condition per experiment. (Scale bars: *B* and *C*, 50 μm.)

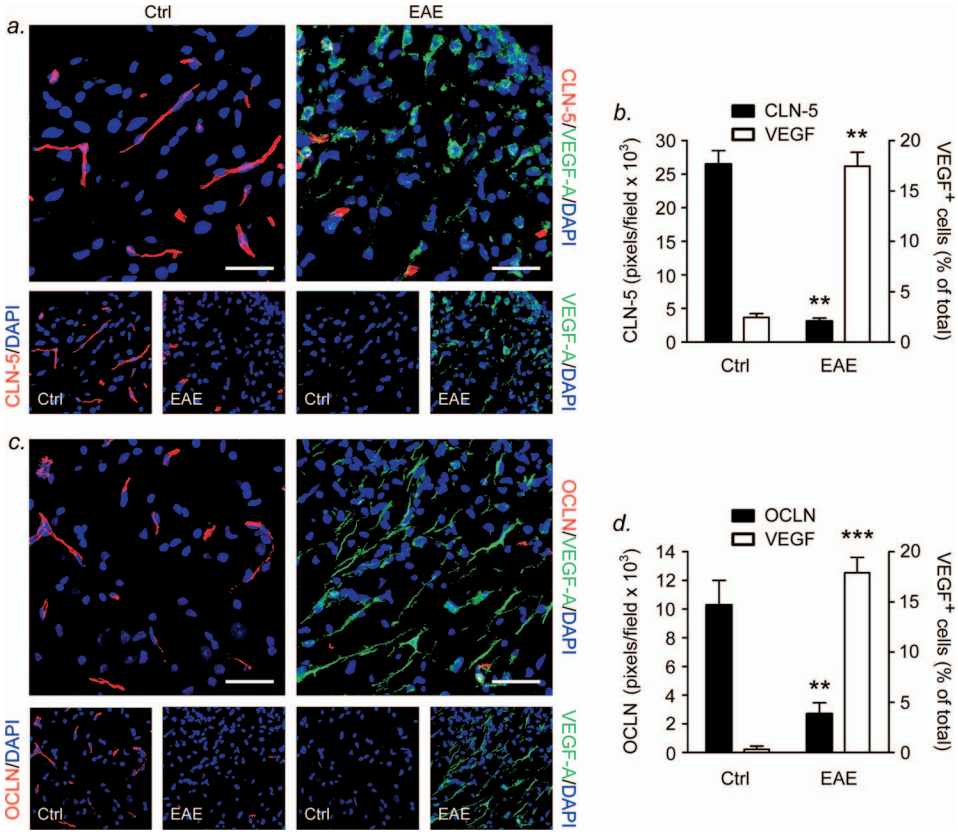

Fig. S2. Up-regulation of VEGF-A accompanies down-regulation of CLN-5 and OCLN in EAE. (*A* and *C*) Confocal Z-series projections of dorsolateral lumbar spinal cord from 10-week C57BL/6 mice with EAE (paraparesis, *Right*) 15–18 d after induction, or age-and sex-matched controls (*Left*), immunostained for VEGF-A plus CLN-5 (*A*) or VEGF-A plus OCLN (*C*). In EAE sections, up-regulation of VEGF-A is accompanied by reduced immunoreactivity for CLN-5 and OCLN. Individual channels are presented below each image for clarity. (*B* and *D*) Morphometric analysis (see *Materials and Methods*) confirms that, in samples from animals with EAE, the number of VEGF$^+$ cells is significantly increased (*B*, $P < 0.01$; *D*, $P < 0.001$, Student *t* test), and that, in the same fields, CLN-5 and OCLN immunoreactivity are significantly reduced (*B*, $P < 0.01$; *D*, $P < 0.01$, Student *t* test). Results are shown from projections from 5 animals with EAE and 5 controls, at least 5 random $\times 20$ fields in 5 sections per animal from the lumbar spinal cord. Data are representative of findings from 3 experiments, 5 animals per condition per experiment. (Scale bars: *A* and *C*, 100 μm.)

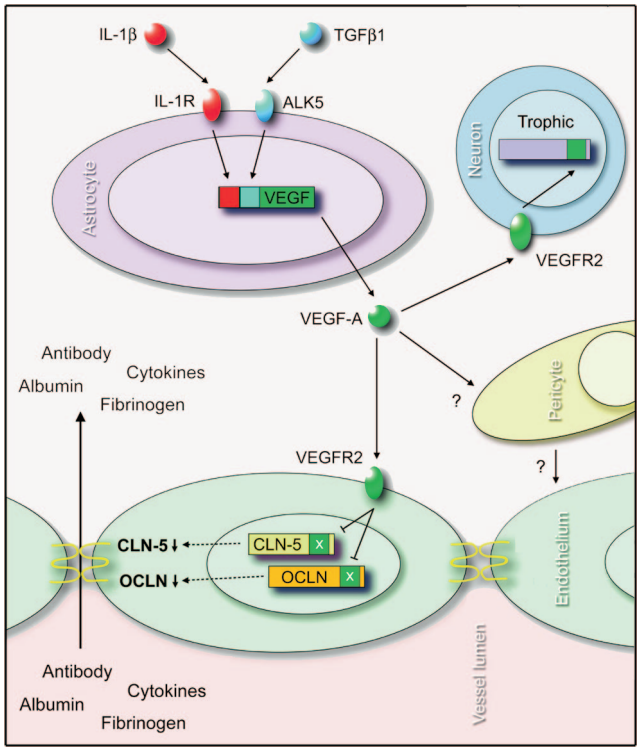

Fig. S3. Proposed model for disruption of CLN-5 and OCLN in CNS inflammation. The inflammatory cytokines IL-1β or TGFβ1 (*Top*) bind to their receptors on astrocytes adjacent to CNS microvessels, activating signal transduction and leading to VEGF-A induction. VEGF-A released from the astrocyte binds to VEGFR2 receptors on BMVECs, activating VEGF signaling and down-regulating CLN-5 and OCLN. Down-regulation of CLN-5 leads to disruption of endothelial tight junctions and BBB breakdown (*Bottom*), allowing accumulation in the CNS parenchyma of antibody, plasma proteins, and cytokines. In addition to its effects on endothelium, VEGF-A also exerts neuroprotective effects on VEGFR2-expressing neurons (*Upper*, *Right*), which would have to be taken into account in any therapeutic approach aimed at the BBB. Pericytes (*Right*) also regulate microvessel structure and trans-endothelial permeability in the CNS. It is not understood how astrocyte-driven and pericyte-mediated effects interact at the BBB.